ELSEVIER

Journal of Power Sources 74 (1998) 117–121

JOURNAL OF POWER SOURCES

A new method for preparing lithiated vanadium oxides and their electrochemical performance in secondary lithium batteries

Aishui Yu [a,*], Naoaki Kumagai [b], Zhaolin Liu [a], Jim Y. Lee [c]

[a] *Institute of Materials Research and Engineering, National University of Singapore, 10 Kent Ridge Crescent, Singapore 119260, Singapore*
[b] *Department of Applied Chemistry and Molecular Sciences, Faculty of Engineering, Iwate University, Morioka 020, Japan*
[c] *Department of Chemical Engineering, National University of Singapore, 10 Kent Ridge Crescent, Singapore 119260, Singapore*

Received 1 December 1997; accepted 16 January 1998

Abstract

This paper describes a new method for preparing lithiated vanadium oxides which are suitable as the cathode material for secondary lithium batteries. Characterization by powder X-ray diffraction (XRD), infrared spectroscopy (IR), scanning electron microscopy (SEM) and thermogravimetric analysis (TGA) shows that these oxides are somewhat structurally different from LiV_3O_8 prepared by the solid-state reaction route, although the starting materials are identical in both cases. The discharge capacity of the oxide is much higher than that of crystalline LiV_3O_8, and can attain 250 mAh g^{-1} at the current density of 0.2 mA cm^{-2}. The specific capacity and the cycling behaviour of these lithiated vanadium oxides are closely related to post-synthesis heat treatment. This suggests that the amount of water bound to the structure determines electrochemical performance of the oxide in secondary lithium batteries.

Keywords: Lithium vanadate; Secondary lithium battery; Cathode material

1. Introduction

Vanadium oxides exist in a number of forms, such as the layered structure and the ReO_3 structure [1,2]. They all have the general formula VO_{2+x}, where x normally varies from 0 to 0.33. Some better known phases in the VO_{2+x} family include VO_2, V_6O_{13}, V_4O_9 and V_3O_7. Corner and edge sharing distorted VO_6 octahedrons are the building blocks in all of them [3–5].

Vanadium oxides have been extensively studied as a cathode material for rechargeable lithium batteries. Among them, V_6O_{13} with the layered structure has attracted much attention since the pioneering work of Christian et al. [6] in 1979. As highly lithiated V_6O_{13} is a poor electronic conductor, most of the follow-up work was dedicated to the improvement of its properties. In particular, doping by Ag, Na, Fe, K cations has received the greatest attention [7–11].

Layered lithiated trivanadate, LiV_3O_8, is an interesting alternative to V_6O_{13} in secondary lithium batteries [12]. Early in its development, Nassau and Murphy [13] had realized the importance of preparation conditions on the ensuing electrochemical properties of LiV_3O_8, particularly in areas such as discharge capacity, rate capability, and cycling behaviour. Improved material performance can be achieved by rapid cooling, effective grinding, hydrothermal technology, substitution of lithium with other monovalent cations such as Na, and K, and proper dehydration of aqueous lithium vanadate gel [14–20].

Recently, two new methods were added to the repertoire, namely the ultrasonic post-treatment of LiV_3O_8 in aqueous solutions and the intercalation of inorganic molecules such as NH_3, H_2O, CO_2 between the LiV_3O_8 interlayers [21,22]. The beneficial effect of inserting a small amount of inorganic molecules between the layers of LiV_3O_8 is believed to cause an expansion of the interlayer spacing that leads to an increase in lithium mobility and a better distribution of Li^+ ions between the layers.

In this work, water molecules are inducted into the LiV_3O_8 structure during synthesis and not through any

* Corresponding author. Fax: +65-872-0785; e-mail: as-yu@imre.org.sg.

0378-7753/98/$19.00

post-synthesis procedure. The products were extensively characterized and evaluated in terms of their performance as the cathode material in secondary lithium batteries.

2. Experimental

2.1. Preparation of lithiated vanadium oxide

Anhydrous Li_2CO_3 and V_2O_5 (Kanto Chemical) were used as the starting materials. Li_2CO_3 and V_2O_5 were mixed in the molar ratio of 1:3 in an agate mortar. The mixture was then transferred to a porcelain crucible and heated to 650°C at the rate of 1°C min^{-1} in a Sibata SCM-200 instrument. After 10 h at 650°C, the reaction melt was quickly quenched in water. The resulting solid was removed by filtration, dried at room temperature, and subsequently heat-treated at different temperatures.

2.2. Characterization of oxide structures

The oxide products were characterized by X-ray diffraction (XRD), thermogravimetric analysis (TGA), infrared spectroscopy (IR), and scanning electron microscopy (SEM). XRD measurements were carried out using a Rigaku Denki Geiger Flux 20B with Cu Kα Radiation. IR spectra were recorded on a Hitachi 2951R spectrophotometer using the KBr disk method. For SEM examination, an Akashi Alpha-10 machine was used. TGA profiles were measured on a Rigaku instrument with a heating rate of 10°C min^{-1}.

2.3. Electrochemical properties of oxides

The fabrication of electrodes and the electrochemical test cell have been previously described [22]. A mixture of oxide and graphite in a weight ratio of 1:1 was compressed on to a nickel net to form the working electrode. The typical cathode loading was about 10 mg cm^{-2} of active material. The electrolyte was a 1 M $LiClO_4$–PC (propylene carbonate) solution, and lithium pellets were used as both the reference and the counter electrodes. The assembly of the electrodes for the test cell was carried out at 25°C in a dry box with an argon atmosphere.

The electrodes were charged and discharged under constant-current control using a HJ-201B instrument (Hokuto Denko). Cyclic voltammograms were measured by connecting the test cell to a HB-501 potentiostat and a HB-104 function generator (Hokuto Denko).

3. Results and discussion

3.1. Structural characterization of lithiated vanadium oxides

The TGA curve of an as-synthesized sample is shown in Fig. 1. The weight loss below 100°C can be attributed to

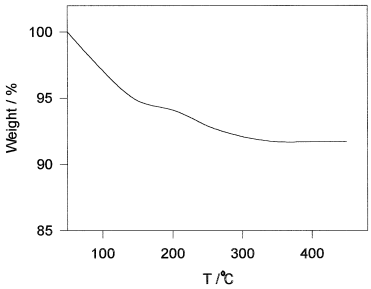

Fig. 1. TGA curves of the as-synthesized lithium vanadium oxide. Heating carried out in air at 10°C min^{-1}.

the removal of loosely-bound water molecules. Some were removed around 150°C, and strongly-bound water could only be removed by continuous heating at 350°C. Based on the TGA results, eight water molecules are calculated to remain in the lithium vanadate structure, and three of them are lost at heating temperature from 100–200°C. The amount of the water in the oxide is higher than that from autoclave or ultrasonic post-treatment in aqueous solution. The temperature required for the complete removal of water is also higher than LiV_3O_8 synthesized otherwise [21,22]. This implies that water molecules which are incorporated by the direct quenching of the reaction melt have higher binding energies with the lithium vanadate host.

The XRD patterns of the as-synthesized oxide and its heat-treated products are given in Fig. 2. These show the structural changes that have occurred during heat-treatment. In comparison with crystalline LiV_3O_8 prepared from a solid-state reaction, additional peaks are found at 18, 20 and 37° and these may arise from new structures induced by the presence of water molecules in LiV_3O_8. Subsequently, these peaks disappear with the increase in the heat-treatment temperature. The XRD patterns of the sample treated at 350°C, at which all the water is removed, are the same as that of crystalline LiV_3O_8, For all samples, there is a noticeable shift of the 2θ of the (100) peak to a lower value at 13.4°. The corresponding d_{100} value of 6.60

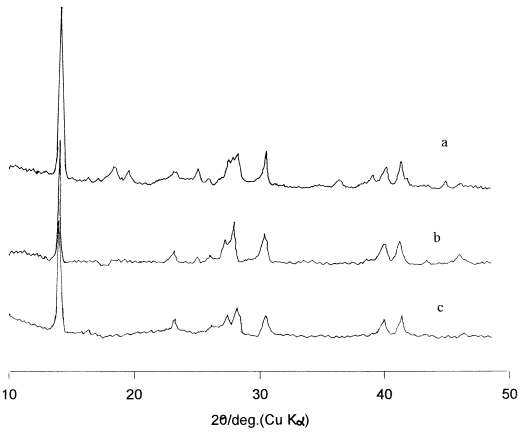

Fig. 2. XRD patterns of lithium vanadium oxides with different heat treatment: (a) no heat treatment; (b) heated at 250°C; (c) heated at 350°C.

Å is higher than the d_{100} value of LiV_3O_8 prepared by conventional means at high temperature (6.36 Å), but is lower than what is possible with autoclave and ultrasonic post-treatment in an aqueous environment [21,22]. The water molecules inducted by the present method are therefore more strongly bound to the oxide lattice than the other two methods. The d_{100} value is also invariant with the increase in heat-treatment temperature. This indicates that the water molecules are not located in the interlayers, but are held closer to the lattice points. The XRD patterns also show an decrease in the full width at half peak (FWHP) with heating, that is, there is some improvement in the crystallinity of the product.

The IR spectra of the as-synthesized and heat-treated oxide samples are shown in Fig. 3. For the former, the IR absorption in the spectral region of 400 to 2000 cm^{-1} is dominated by four bands at 1600, 1020, 910 and 740 cm^{-1}, respectively. When this data is compared with LiV_3O_8 from solid-state reactions, where major IR bands corresponding to V = O and V–O–V vibrations are located at 996, 816 and 712 cm^{-1}, respectively. The 1600 cm^{-1} band for the as-synthesized oxide can be assigned to the presence of residual water in the structure. The intensity of this band decreases with the heat-treatment temperature and disappears completely at 250°C. The oxide treated at 350°C gives the same IR responses as that of crystalline LiV_3O_8, and suggests that it is almost iso-structural with the latter.

The scanning electron micrographs of the various oxides are shown in Fig. 4. It is obvious that heat treatment has caused a change in the oxide crystallinity and morphology. The oxide without any heat treatment (Fig. 4a) is somewhat amorphous and consists of an agglomeration of small particles. Heating at 150°C (Fig. 4b), transforms the oxide into needle-like polycrystallites about 1 μm in diameter. The oxide treated at 350°C is monoclinic and morphologically similar to the product from a high-temperature, solid-state reaction. The increase in crystallinity with temperature is therefore in good agreement with the XRD measurements.

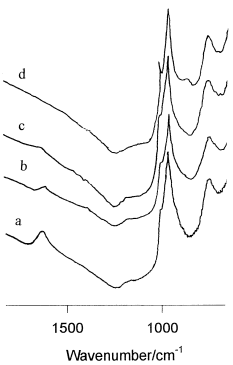

Fig. 3. Infrared spectra of lithium vanadium oxides with different heat treatment: (a) no heat treatment; (b) heated to 150°C; (c) heated to 250°C; (d) heated to 350°C.

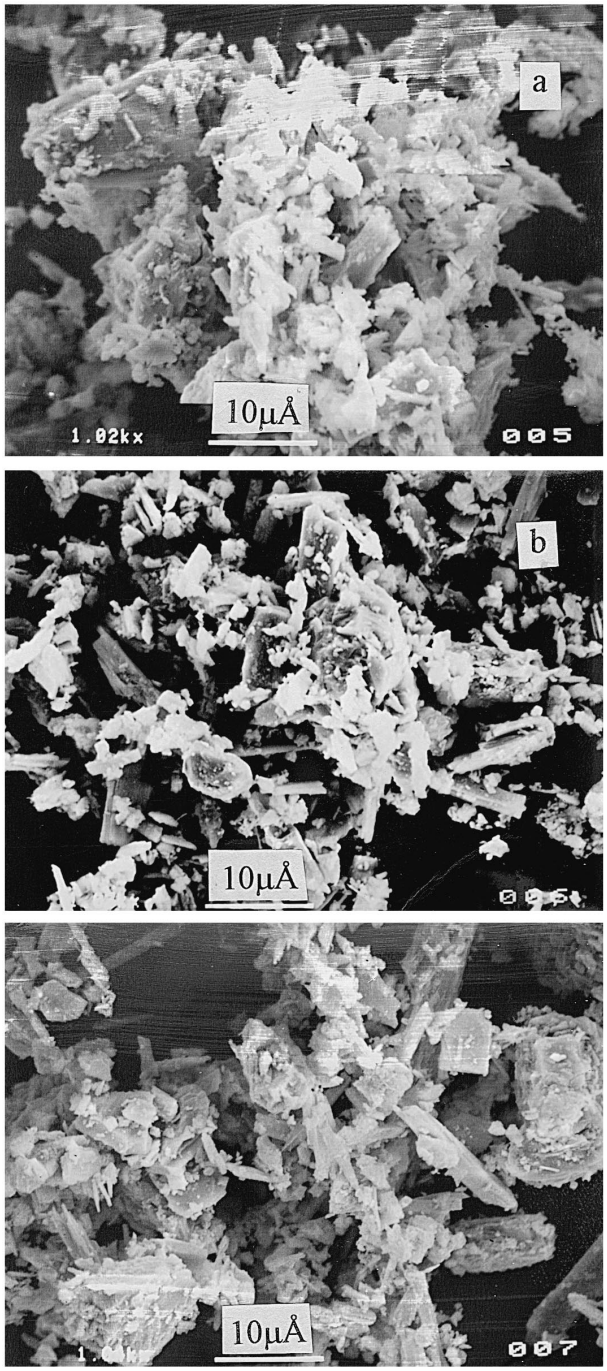

Fig. 4. Scanning electron micrographs of several lithium vanadium oxides: (a) no heat treatment; (b) heated to 150°C; (c) heated to 350°C.

3.2. Electrochemical characteristics of lithium vanadium oxide cathodes in secondary test cells

Typical cyclic voltammograms of lithiated vanadium oxide and its heat-treated product at 350°C are shown in Fig. 5. The voltammograms were measured at a scan rate

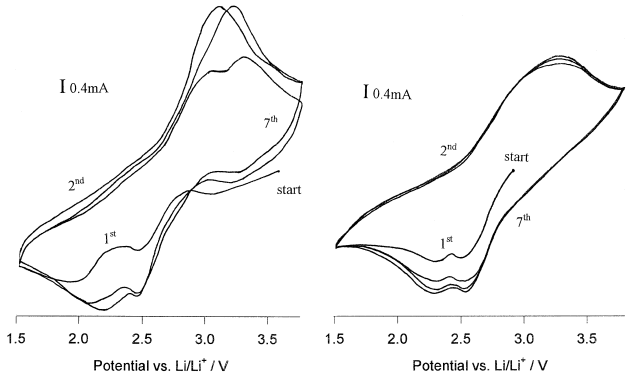

Fig. 5. Typical cyclic voltammograms of lithium vanadium oxides at 0.2 mV s^{-1}: (a) no heat treatment; (b) heated to 350°C.

of 0.2 mV s^{-1} in the potential range from 3.8 to 1.7 V at room temperature. The first voltammograms are rather different from the rest; some structural modifications have probably taken place during the first charge and discharge operations. For the non heat-treated oxide, the main cathodic peaks are located at 2.5 and 2.2 V vs. Li^+/Li, with anodic peaks at 3.3 and 3.0 and 3.7 V. The heat-treated oxides also have similar general voltammetric features, but the peak position and the peak intensity are different, and there is only one anodic peak at 3.2 V. It is tempting to attribute such difference to the total absence of water molecules after heat treatment. The 2nd to 7th cycles of the voltammograms are nearly identical and display good reversibility at the scan rate of 0.2 mV s^{-1}. Lithium-ion intercalation and de-intercalation are therefore made easier after electrode conditioning by an initial charge and discharge.

The effect of heat-treatment temperature on the electrochemical behaviour of the oxides can be deduced from the series of discharge curves shown in Fig. 6. Another perspective is provided by the plots of initial discharge capacity (drawn at the current density of 0.2 mA cm^{-2}) against cycle number in Fig. 7. It is found that the non-heat-treated oxide has the highest initial discharge capacity among all oxides. Its value of 250 mAh g^{-1} is considerably higher than the specific capacity of crystalline LiV_3O_8 (175 mAh g^{-1}). However, with the same discharge current, the discharge voltage is somewhat lower than that of crystalline LiV_3O_8 [22]. The presence of bound water molecules in the host lattice should be a contributing factor. Interestingly, the best cycle ability is delivered by the oxide treated at 250°C. This implies that the presence of a small amount of water is beneficial to the reversibility of lithium-ion intercalation and de-intercalation. A similar trend has also been observed for hydrothermally synthe-

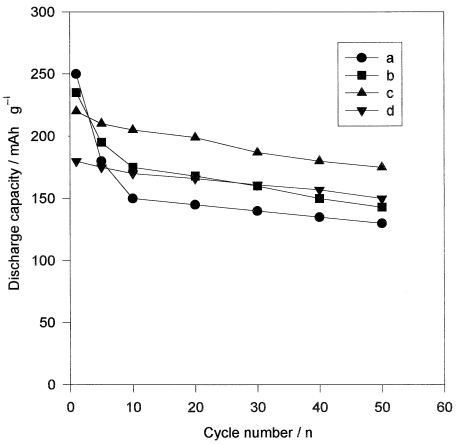

Fig. 7. Changes in discharge capacity as a function of cycle number of various lithium vanadium oxides. Electrodes cycled at a constant-current density of 0.2 mA cm^{-2}: (a) no heat treatment; (b) heated to 150°C; (c) heated to 250°C; (d) heated to 350°C.

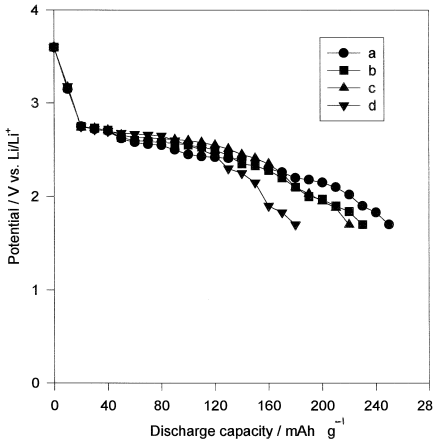

Fig. 6. Initial discharge curves of several lithium vanadium oxides at 0.2 mA cm^{-2}: (a) no heat treatment; (b) heated to 150°C; (c) heated to 250°C; (d) heated to 350°C.

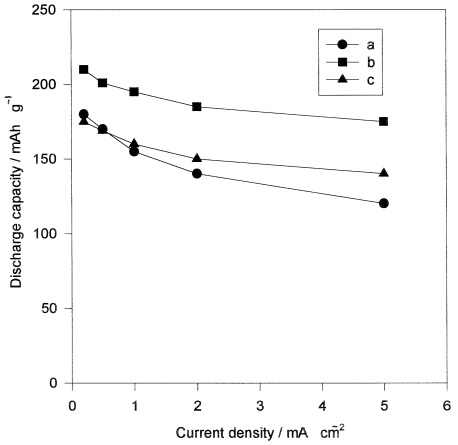

Fig. 8. Discharge capacity on 10th cycle as a function of current density for several lithium vanadium oxides: (a) no heat treatment; (b) heated to 250°C; (c) heated to 350°C.

sized and ultrasonically treated LiV_3O_8 [21,22]. Hence, irrespective of the inherent differences in composition, crystal structure, specific surface area and morphology of lithiated vanadium oxides prepared by various methods, a small amount of water bounded to the host structure will provide a higher initial discharge capacity and a better cycle life.

The rate capability of oxides treated at different temperatures was examined with current densities ranging from 0.2 to 5 mA cm^{-2}. From the plot of discharge capacity on the 10th cycle is plotted against the current density in Fig. 8. It can be seen that heat treatment at 250°C results in the highest discharge capacity. Even at the high current drain of 5 mA cm^{-2}, a discharge capacity of 180 mAh g^{-1} can still be sustained. This is about 50% more than that provided by crystalline LiV_3O_8 under similar conditions [22]. The improvement can be traced to the structural difference between these two forms of LiV_3O_8. The structure arising from the presence of small amount of strongly bound water molecules is conducive to lithium mobility and, hence, a more uniform distribution of lithium during intercalation.

4. Conclusions

Water molecules can be incorporated in the lithiated vanadium oxide structure through rapid quenching of the reaction melt from a high-temperature, solid-state reaction in water. The water molecules can still be removed by heating above 350°C and the resulting oxide is no different from crystalline LiV_3O_8. Heat treatment at an intermediate temperature of 250°C produces a partially dehydrated oxide which gives higher discharge capacity and better cycling performance than completely dehydrated and crystalline LiV_3O_8. The presence of a small amount of strongly bound water in the host lattice can lead to a larger interlayer spacing which enhances lithium mobility and the uniform distribution of Li^+ ions between the layers.

Acknowledgements

The authors would like to express their thanks to Mrs. N. Kumagai and Mr. S. Saito for their experimental assistance.

References

[1] K. Kawashima, K. Kosuge, S. Kashi, Chem. Lett. 1131 (1995) .
[2] C. Lampe-Onnerud, J.O. Thomas, M. Hardgrave, S.Y. de-Anderson, J. Electrochem. Soc. 142 (1995) 3648.
[3] K. Wilhelmi, K. Waltersson, L. Kihlborg, Acta Chem. Scand. 25 (1971) 2675.
[4] F. Theobald, R. Cabala, J. Bernard, J. Solid State Chem. 17 (1976) 431.
[5] G. Grymonprez, L. Fiermans, J. Vennik, Acta Crystallogr. 33A (1977) 834.
[6] P.A. Christian, F.J. Disalvo, D.W. Murphy, US Pat. 4,228,226, 1980.
[7] J. Pereira-Ramos, L. Znaidi, N. Buffier, R. Messiua, Solid State Ionics 28–30 (1988) 886.
[8] N. Buffier, L. Znaidi, M. Huber, Mater. Res. Bull. 25 (1990) 705.
[9] S. Maingot, Ph. Deniard, N. Buffier, J.P. Pereira-Ramos, A. Kahn-Harari, R. Brec, P. Willmann, J. Power Sources 54 (1995) 342.
[10] K. West, A.M. Crespi, J. Power Sources 54 (1995) 334.
[11] E.S. Takeuchi, W.C. Thiebolt III, J. Electrochem. Soc. 135 (1988) 2691.
[12] J.O. Besenhard, R. Schöhorn, J. Power Sources, Vol. 1, 1996/1997, 267.
[13] K. Nassau, D.W. Murphy, J. Non-Cryst. Solids 44 (1981) 297.
[14] K. West, B. Zachau-Christiansen, M.J.L. Qstergard, T. Jacobsen, J. Power Sources 20 (1987) 165.
[15] G. Pistoia, M. Pasquali, Y. Geronov, V. Manev, R.V. Moshtev, J. Power Sources 27 (1989) 35.
[16] G. Pistoia, M. Pasquali, G. Wang, L. Li, J. Electrochem. Soc. 137 (1990) 2365.
[17] G. Pistoia, G. Wang, D. Zane, Solid State Ionics 76 (1995) 285.
[18] M. Pasquali, G. Pistoia, Electrochim. Acta 36 (1991) 1549.
[19] K. West, B. Zachau-Christiansen, S. Skaarup, Y. Saidi, J. Barker, I.I. Olsen, R. Pynenburg, R. Koksbang, J. Electrochem. Soc. 143 (1996) 820.
[20] N. Kumagai, A. Yu, K. West, J. Appl. Electrochem. 27 (1997) 953.
[21] M. Manev, A. Momchilor, A. Nassalevska, G. Pistoia, M. Pasquali, J. Power Sources 54 (1995) 501.
[22] N. Kumagai, A. Yu, J. Electrochem. Soc. 144 (1997) 830.